

Strain effect on the electronic and optical properties of 2D Tetrahexcarbon: a DFT-based study

D. M. Hoat, Shirin Amirian, Hamidreza Alborznia, Amel Laref, A. H. Reshak & Mosayeb Naseri

Indian Journal of Physics

ISSN 0973-1458

Indian J Phys

DOI 10.1007/s12648-020-01913-1



Your article is protected by copyright and all rights are held exclusively by Indian Association for the Cultivation of Science. This e-offprint is for personal use only and shall not be self-archived in electronic repositories. If you wish to self-archive your article, please use the accepted manuscript version for posting on your own website. You may further deposit the accepted manuscript version in any repository, provided it is only made publicly available 12 months after official publication or later and provided acknowledgement is given to the original source of publication and a link is inserted to the published article on Springer's website. The link must be accompanied by the following text: "The final publication is available at link.springer.com".

Strain effect on the electronic and optical properties of 2D Tetrahexcarbon: a DFT-based study

D M Hoat^{1,2}, S Amirian³, H Alborznia³, A Laref⁴, A H Reshak^{5,6,7} and M Naseri^{3*} 

¹Computational Laboratory for Advanced Materials and Structures, Advanced Institute of Materials Science, Ton Duc Thang University, Ho Chi Minh City, Vietnam

²Faculty of Applied Sciences, Ton Duc Thang University, Ho Chi Minh City, Vietnam

³Department of Physics, Kermanshah Branch, Islamic Azad University, Kermanshah, Iran

⁴Physics Department, Faculty of Science, King Saud University, Riyadh, Saudi Arabia

⁵Physics Department, College of Science, University of Basrah, Basrah, Iraq

⁶Department of Instrumentation and Control Engineering, Faculty of Mechanical Engineering, CTU in Prague, Technicka 4, Prague 6 166 07, Czech Republic

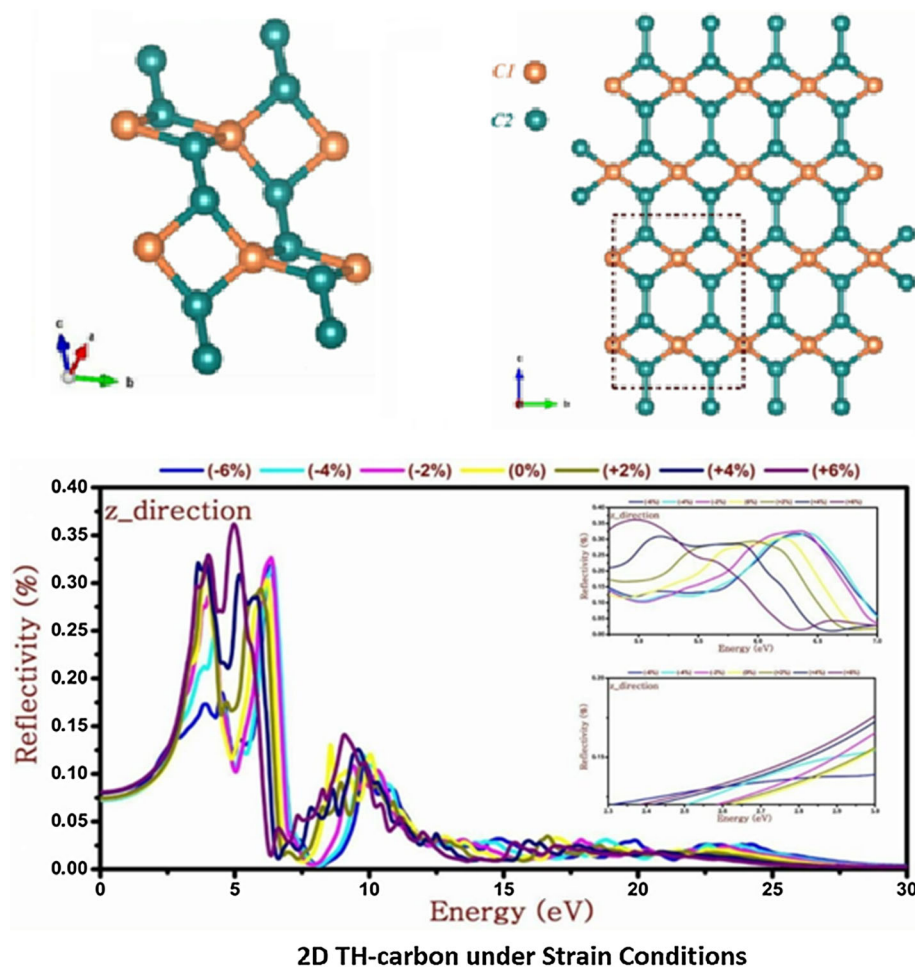
⁷Center of Excellence Geopolymer and Green Technology, School of Material Engineering, University Malaysia Perlis, 01007 Kangar, Perlis, Malaysia

Received: 02 April 2020 / Accepted: 14 August 2020

Abstract: A new two-dimensional (2D) carbon allotrope, namely Tetrahexcarbon (TH-carbon) semiconductor monolayer with a direct band gap resides in the visible region of the electromagnetic spectra, has been recently proposed theoretically. Herein, the influences of biaxial strains on the electrical and optical aspects of 2D TH-carbon are computationally investigated. To this end, first-principles calculations based on the properties of the density functional theory were employed. According to our simulations, the electronic and optical properties of 2D TH-carbon are effectively sensitive to the external strain effects. This obtained strain sensitivity suggests that this 2D material could be a promising material for usage in new electronic technologies.

*Corresponding author, E-mail: m.naseri@iauksh.ac.ir

Graphic abstract



Keywords: First-principles calculations; TH-carbon monolayer; Electronic Properties; Optical properties; Strain effect

1. Introduction

Since the discovery of graphene [1], the two-dimensional (2D) carbon allotrope with unusual dynamical, electronic and optical properties [2–7] and promising application for designing electronic and optoelectronic devices, and many investigations have been conducted to find new possible 2D monolayer materials [2–13]. In this way, a variety of new carbon-based materials have been attained or predicted [14–22].

Among the carbon allotropes, 2D pure hexagon graphene which is a gapless semiconductor [23] and the bulk pentagon carbon allotrope, namely T12-carbon [24], which is a wide gap semiconductor, have attracted great interest due to their exceptional physical aspects. Inspired from T12-carbon, by using density functional theory (DFT), a new 2D monolayer allotrope of carbon with pentagon

crystal configuration called penta-graphene has been proposed [25]. Short after, the electronic and optical properties of penta-graphene have been widely investigated and it has been shown that its electronic and optical properties can be effectively modulated by applying strain effects [26]. Moreover, by using which can be derived from penta-graphene structure, a new stable allotrope of carbon called Tetrahexcarbon (TH-carbon) [21] is predicted. It has been found that the new proposed carbon allotrope, i.e., TH-carbon, shows interesting characteristics such as a direct band gap, remarkable electrical properties and high electron mobility suggest it for usage in nanoelectronics and optoelectronic devices. Therefore, it is worth to conduct more investigating on its physical aspects.

It is well known that the physical properties of a 2D material may be engineered by different methods such as chemical functionalizing [27–29], doping [30–32],

mechanical loading [33–35] or strain engineering [36–41]. More recently, the possibility of manipulating the physical and chemical properties of 2D TH-carbon monolayer by controlled hydrogenation has been systematically studied by Kilik et al. [42]. In their investigation, Kilik et al. accessed the pristine TH-carbon and its various hydrogenated configurations and show the phononic and electronic band gap of the TH-carbon can be tuned by hydrogenation and a direct–indirect–direct band gap transitions have been also observed.

In the field of 2D monolayer materials investigation, the strain engineering has recently attracted a lot of interest from many researchers. The main goal of strain effects investigations is to get accurate insights into the effects of mechanical strains on the electronic, optical and photonic performance of 2D materials and to establish high-performance 2D-material-based devices. The strain effects can be occurred not only by an external strain but also via the mismatch between lattice constants of the synthesized material and substrate; therefore, the impact of the strain on the electronic and optical features of a newly designed 2D material is essentially an important task.

In this letter, by employing first-principles calculations based on the state of the density functional theory (DFT), the optimized structure data of TH-carbon unit cell are acquired by means of two approximation methods, i.e., Perdew–Burke–Ernzerhof (PBE) [43], and Heyd–Scuseria–Ernzerhof (HSE06) hybrid functional theory [44] level of theories. After that, the electronic and optical aspects of TH-carbon under biaxial stress and strain condition are analyzed and the outcome results will be beneficial for next experimental attempts for usage to design the optoelectronic applications.

2. Computational methods and details

To investigate the electronic and optical aspects, first-principles calculations in the framework of DFT, as embodied in WIEN2k computational code [45], have been used. In these calculations, the Kohn–Sham wave functions are expanded by non-spin-polarized full potential linear augmented plane waves plus local orbital (FP-LAPW + LO) method and the exchange–correlation term is represented by generalized gradient approximation in the form of Perdew–Burke–Ernzerhof (GGA-PBE) [43] theory. In order to procure accurate band gaps, the electronic band structures are also examined by Heyd–Scuseria–Ernzerhof (HSE06) hybrid functional theory [44]. For electronic and optical calculations, using the Monkhorst–Pack approximation [46], k-point meshes of $12 \times 12 \times 1$ and $25 \times 25 \times 1$ are selected, respectively. Furthermore, the computational input parameters of $R_{\text{MT}}K_{\text{max}} = 7$, $G_{\text{max}} =$

$14 R_y^{1/2}$, $l_{\text{max}} = 10$ are undertaken, in which the separation energy of $-8 R_y$ is chosen to separate the core from the valence electrons. Finally, in the optical properties evaluation, the Kramers–Kronig relations [47] and the random phase approximation (RPA) method [48] are applied.

3. Results and discussion

TH-carbon is a new stable allotrope of carbon which is derived from penta-graphene. A unit cell of a 2D TH-carbon monolayer is shown in Fig. 1. In a unit cell of a TH-carbon monolayer, there are different hybrid orbitals with two kinds of carbon atoms (C1 and C2), and the structure is formed by combination of sp^2 and sp^3 -hybridized carbon atoms [21]. A 2D TH-carbon monolayer structure from different views is shown in Fig. 1(a)–(c).

To obtain the optimized lattice constants of the TH-carbon, the Brich–Murnaghan [49] thermodynamically equation state is employed, which is indicated as:

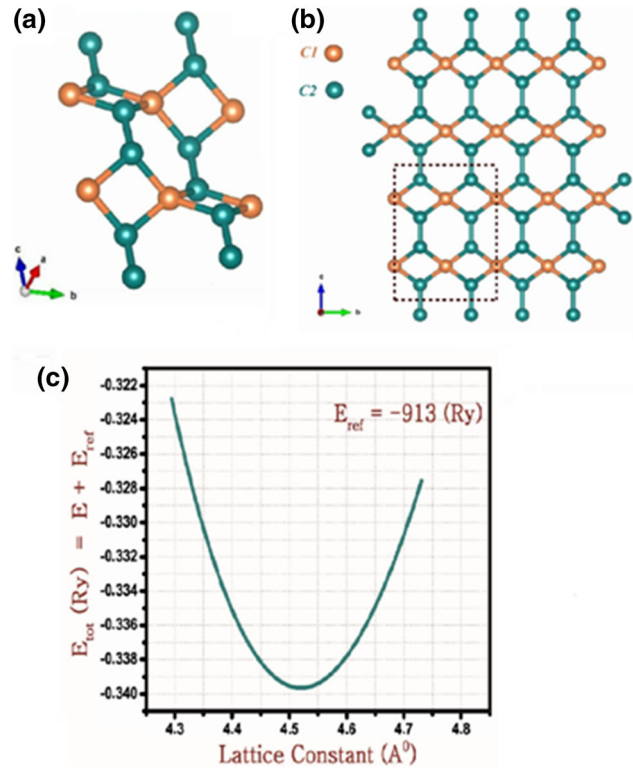


Fig. 1 (a) A unit cell of the TH-carbon monolayer, (b) a supercell of the TH-carbon monolayer and (c) the energy vs volume of a unit cell of the TH-carbon monolayer

$$E(V) = E_0 + \frac{9B_0V_0}{16} \left\{ \left[\left(\frac{V_0}{V} \right)^{2/3} - 1 \right]^3 B'_0 \right\} + \frac{9B_0V_0}{16} \left\{ \left[\left(\frac{V_0}{V} \right)^{2/3} - 1 \right]^2 \left[6 - 4 \left(\frac{V_0}{V} \right)^{2/3} \right] \right\} \quad (1)$$

where B'_0 is the derivative of the bulk modulus with respect to pressure, and B_0 is the bulk modulus without pressure. V_0 is the initial considered volume, and V is the deformed volume. By using the above equation, the energy of unit cell versus the unit cell volume can be calculated. In this scheme, the optimized volume of the optimized unit cell is demonstrated by the minimum point of the obtained curve. Consequently, by using the obtained volume for the optimized unit cell, the optimized lattice constants can be simply calculated. The energy versus the lattice constant of a unit cell of the TH-carbon is plotted in Fig. 1(c).

Based on our calculation, the optimized lattice parameters of $a = 4.52\text{\AA}$ and $b = 6.10\text{\AA}$ were obtained which are in a good agreement with those reported in previous works [21, 42].

Now, let us calculate the cohesive energy of the 2D TH-carbon to validate its stability. The cohesive energy of TH-carbon/unit cell can be written as:

$$E_{\text{coh}} = (mE_C - E_{\text{TH-C}}^{\text{total}})/m \quad (2)$$

where $E_{\text{TH-C}}$ is total energy of TH-carbon, E_C is isolated energy of carbon atom and m refers to the number of carbon atoms in each TH-carbon unit cell. In this calculation, a simple cubic cell with lattice parameters of 15\AA consisting of a carbon atom at its center is considered to find the energy of the carbon atom. According to our calculations, the cohesive energy is obtained for TH-carbon with value of 7.97 eV/atom , indicating the stability of this structure.

To investigate the electronic and optical characters of the monolayer under strain conditions, we first examined the band structures and the density of states of the strain-free structure. Based on our calculation, the optimized 2D TH-carbon is a direct semiconductor with a band gap of around 1.65 eV (2.662 eV) obtained by using PBE (HSE06) approximation as its valence band maximum (VBM), and conduction band minimum (CBM) is located at Γ point. Figure 2 illustrates the band structure and the total density of states (TDOS) for the pristine TH-carbon monolayer. Figure 3 shows the partial density of states (PDOS) of the strain-free TH-carbon. As shown in Fig. 3, it was found that both VBM and CBM for the proposed TH-carbon monolayer semiconductor are mainly contributed by the C1-2p and C2-2p electrons.

To understand the optical properties of the monolayer, we first calculated the complex dielectric function of the material. It is well known that by having the complex dielectric function, all other optical parameters can be simply derived. The complex dielectric function is given by the following equation:

$$\varepsilon(\omega) = \varepsilon_1(\omega) + i\varepsilon_2(\omega) \quad (3)$$

Here, $\varepsilon_1(\omega)$ and $\varepsilon_2(\omega)$ are the real and imaginary parts of the function. This function describes the process of light propagation through the material. Positive value for $\varepsilon_1(\omega)$ reveals the light absorption property of the material at a given frequency. On the other hand, the imaginary part of the dielectric function refers to the Ohmic resistance of the material, i.e., a pure dielectric exhibits zero value for the imaginary part of dielectric function.

The imaginary part of the complex dielectric function can be obtained from the matrix element between the occupied and unoccupied states [50, 51],

$$\varepsilon_{\alpha\beta}^{(2)}(\omega) = \frac{4\pi^2 e^2}{m^2 \omega^2} \sum_{if} \int \frac{2d^3k}{(2\pi)^3} \{ |\langle i_k | P_\alpha | f_i \rangle|^2 f_i^k (1 - f_f^k) \delta(E_f^k - E_i^k - \hbar\omega) \}. \quad (4)$$

Here, i and f present initial and final states, respectively, and E_i^k refers to the corresponding eigenvalue, f_i^k indicates the Fermi distribution and P_α indicates the α as component of the momentum operator. Having the imaginary part of the complex dielectric function, one can simply calculate the real part of the function, $\varepsilon_1(\omega)$, by the Kramers-Kronig relationship

$$\varepsilon_{\alpha\beta}^{(1)}(\omega) = \delta_{\alpha\beta} \frac{2}{\pi} P_r \cdot \int_0^\infty \frac{\varepsilon_{\alpha\beta}^{(2)}(\omega')}{(\omega')^2 - (\omega)^2} d(\omega'). \quad (5)$$

Here, P_r refers to the momentum matrix element between α and β bands with the same crystal momentum K (Cauchy principal value).

In Fig. 4, the imaginary and real parts of the complex dielectric function, the absorption coefficient and the reflectivity of the strain-free TH-carbon, in X and Z polarization direction, are plotted. The static dielectric function, $\varepsilon_1(0)$, which is an important quantity representing the dielectric response to the static electric field, is calculated as $\varepsilon_1(0) \approx 3.05$. Also, $\varepsilon_1(\infty)$ describes the response of the material to the high-energy photons which is calculated as

$\varepsilon_1(\infty) \approx 0.8$. As shown in Fig. 4, the remarkable peaks of both real and imaginary parts of the complex dielectric function occur at visible region of the electromagnetic spectra. In more detail, the main peak of the real dielectric function appears at $E = 3.28\text{ eV}$ with the value of 6.5 , and the main peak of the imaginary dielectric functions is at

Fig. 2 The band structures (PBE and HSE06 method) and total DOS (PBE method) of optimized TH-carbon

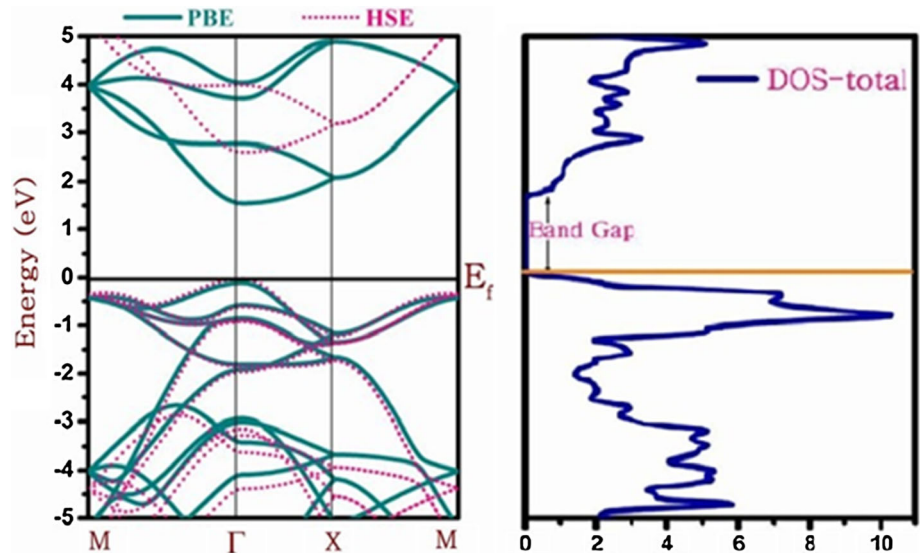
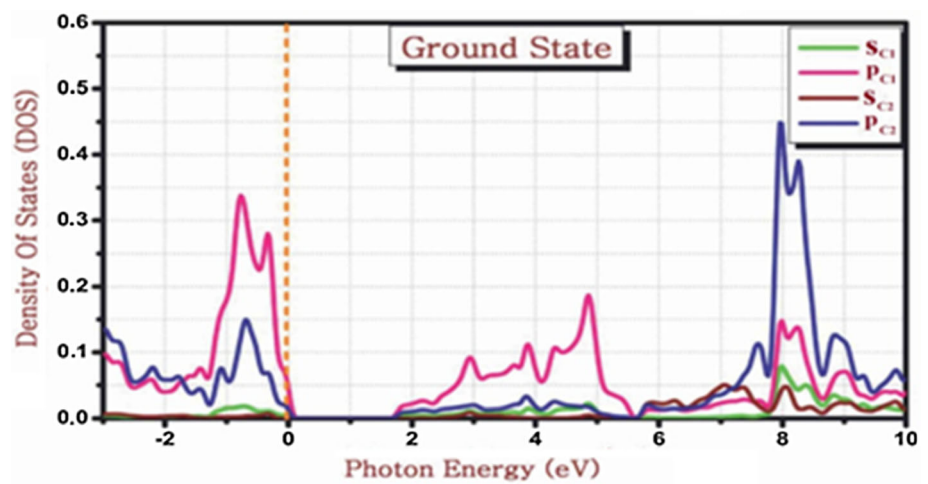


Fig. 3 The partial DOS of TH-carbon crystal in free states



$E = 3.82$ eV with the value of 7.4. The real and imaginary parts of the complex dielectric function for the 2D TH-carbon including more details are given in Fig. 4 (left panel). Furthermore, the absorption and the reflectivity of the TH-carbon monolayer are shown in Fig. 4 (right panel). It is clear that for perpendicular polarization, the monolayer shows a remarkable absorption peak appears at the border of the visible region of the electromagnetic spectra. As shown in Fig. 4 (right panel), the first main peak of the absorption curve appears at $E = 3.93$ eV with the absorption value of $66 \times 10^4 \text{ cm}^{-1}$. However, another remarkable peak appears at $E = 5.70$ eV with the absorption value of about $74 \times 10^4 \text{ cm}^{-1}$. Moreover, as shown in Fig. 4 (right panel), the first significant reflectivity peak occurs at 3.90 eV with the reflection of about 33%. The absorption and reflectivity of the 2D TH-carbon including more details are given in Fig. 4 (right panel).

Next, the electronic and optical aspects of TH-carbon under biaxial strain conditions are investigated. First, let us evaluate the influences of strains on the total energy and band gap of the monolayer.

The band structures of the TH-carbon under biaxial stress and strain conditions of the energy band structures are given in Fig. 5. As shown in Fig. 5, under tensile strain conditions, the band gap first decreases slightly (up to 4% tensile strain), and then, it increases, while it remains direct as its VBM, and CBM remains at Γ point. To be more precise, for the case of 2%, 4% and 6% tensile strains the band gap of 1.622, 1.614 and 1.657 eV was obtained, respectively. On the other hand, by applying biaxial compressive strains, the direct band gap of the monolayer first increases (up to 2% compressive strain) and then it decreases as its values for 2%, 4% and 6% compressive strains are 1.720 eV, 1.515 and 1.107 eV, respectively. The variation of the band gap and total energy of a unit cell of

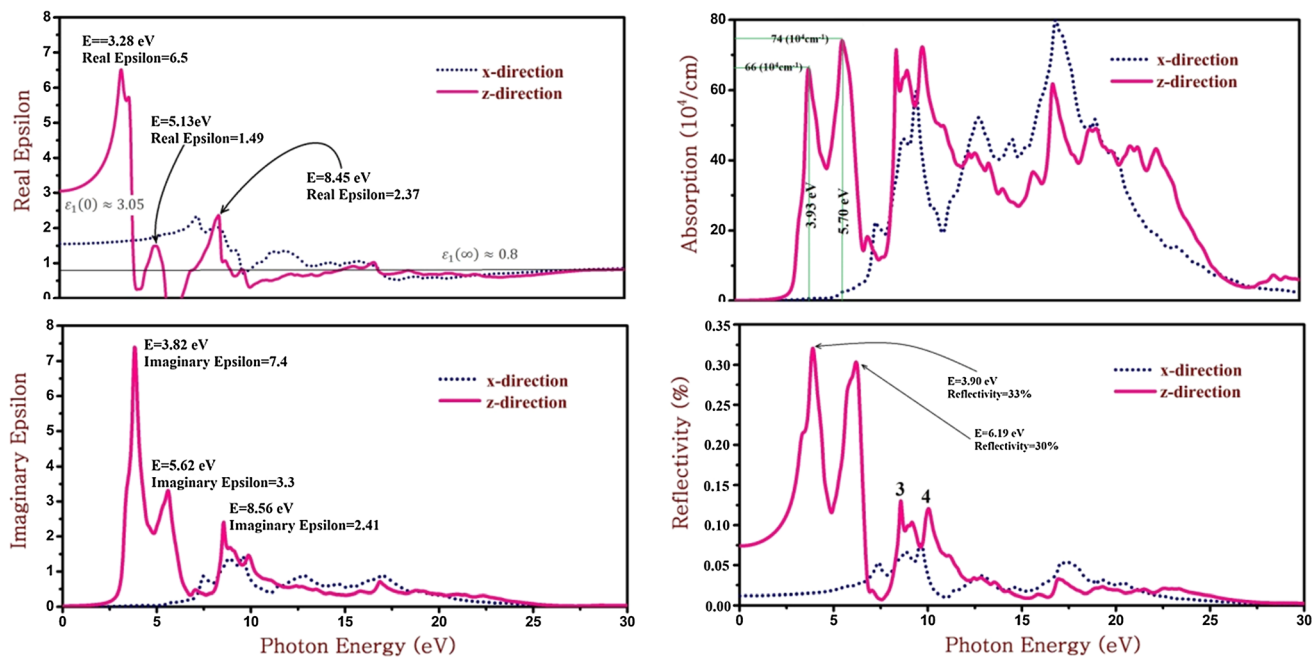


Fig. 4 The imaginary and real parts of the complex dielectric function (left panel figures) and the absorption and the reflectivity coefficient (right panel) of the strain-free TH-carbon in X and Z polarization direction are plotted

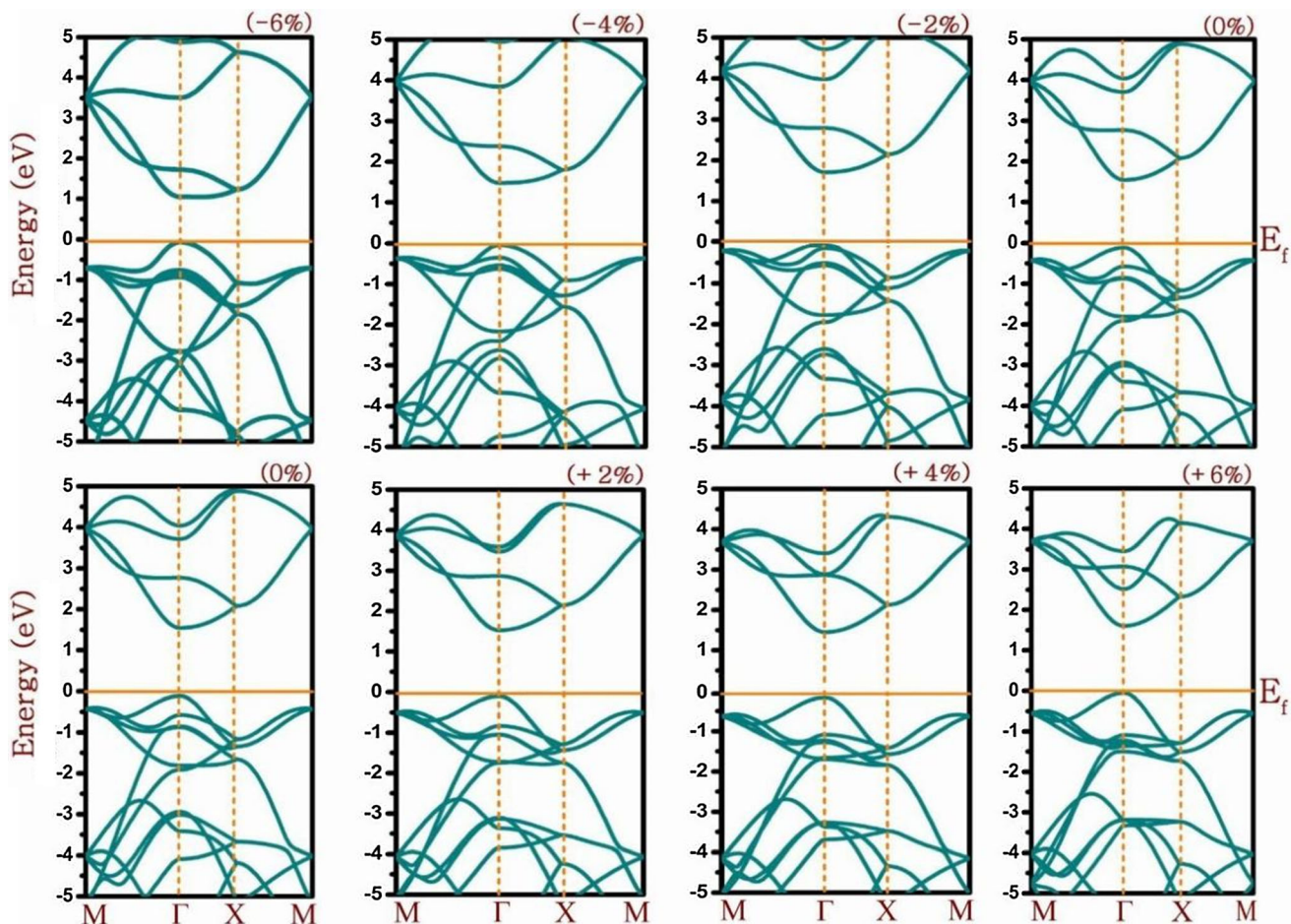


Fig. 5 The energy band structure plots of the TH-carbon under biaxial stress and strain condition calculated by PBE level of theory

Fig. 6 The band gap and total energy of TH-carbon under strain and stress

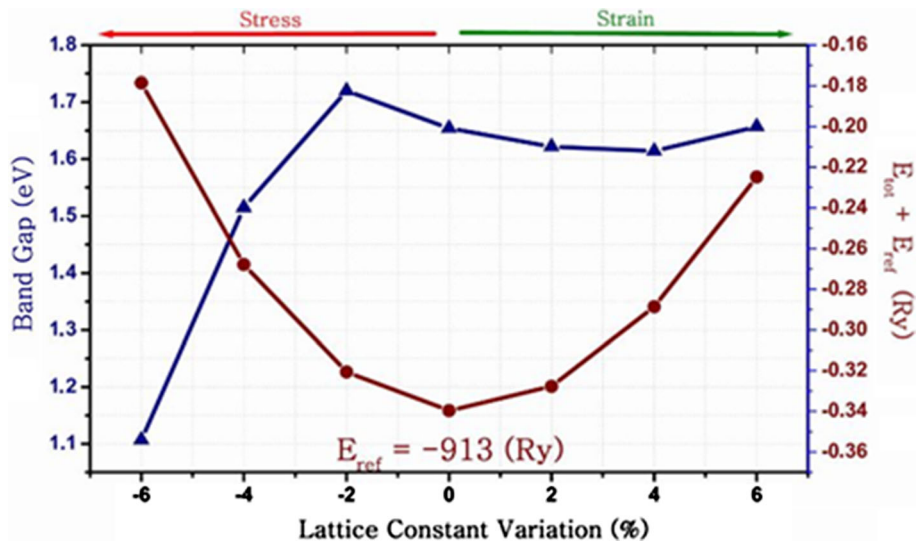
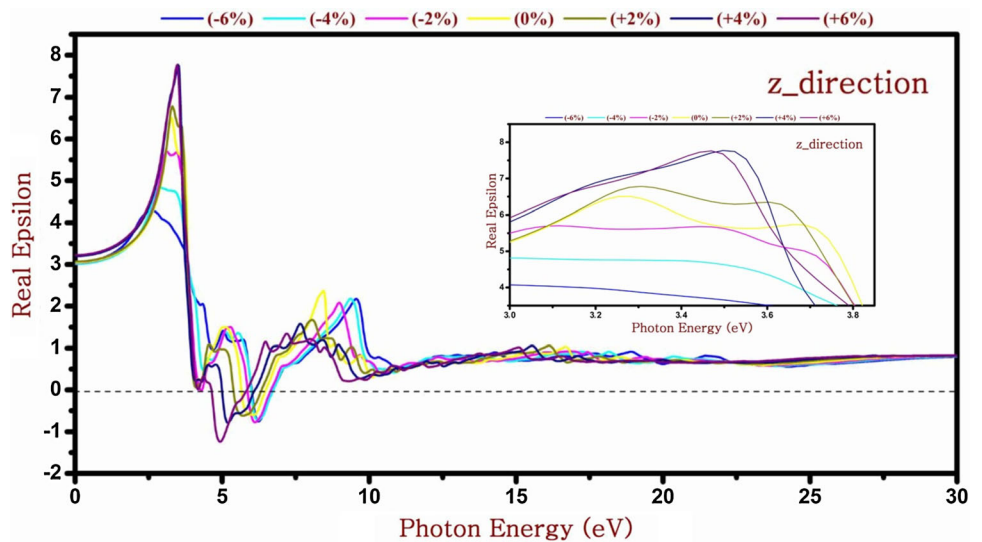


Table 1 Structural data, band gap, total energy and energy of strain for TH-carbon in this work

Stress and strain (%)	-6	-4	-2	0	2	4	6
a (\AA^0)	4.25	4.34	4.43	4.52	4.61	4.70	4.79
b (\AA^0)	5.72	5.84	5.96	6.10	6.21	6.33	6.45
Band gap-PBE	1.11	1.52	1.72	1.65	1.62	1.61	1.66
Band gap-HSE06	2.24	2.66	2.74	2.66	2.62	2.60	2.63
Total energy	-913.1785	-913.2678	-913.3206	-913.3396	-913.3277	-913.2886	-913.2248
E_S (eV/atom)	0.01343	0.00598	0.00158	0	0.00099	0.00425	0.00956

Fig. 7 The real part plot of the dielectric function of TH-carbon under stress and strain



2D TH-carbon is plotted in Fig. 6. Table 1 summarizes the calculated structural and electrical properties of 2D TH-carbon under strain conditions.

Finally, we investigate the optical properties of the 2D TH-carbon monolayer under different strains varying from

-6% compressive strains to 6% tensile strain. The real and imaginary spectra of the complex dielectric function of the 2D TH-carbon monolayer in Z direction are plotted in Figs. 7 and 8, respectively. According to Fig. 7, for the strain-free structure, the main peak of the real part of the

Fig. 8 The imaginary part plot of the dielectric function of TH-carbon under stress and strain

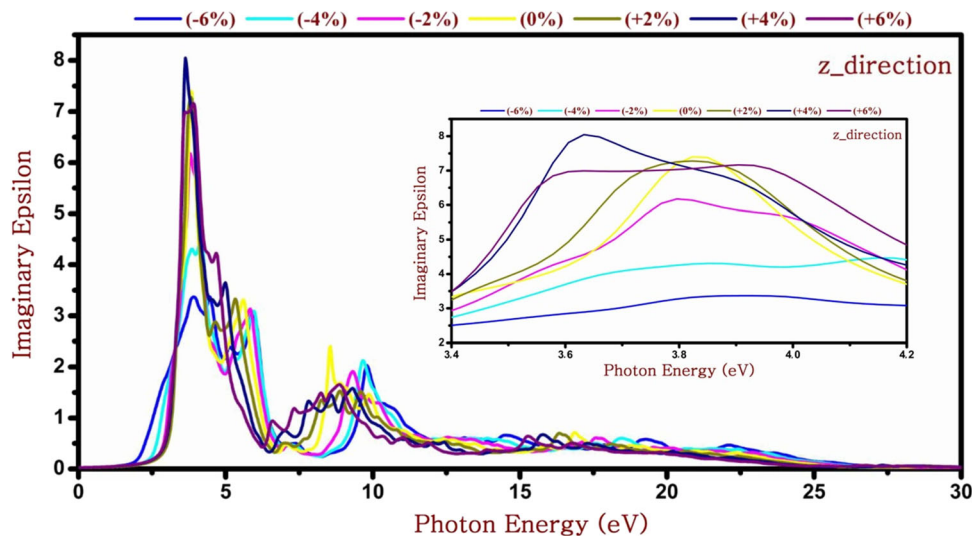
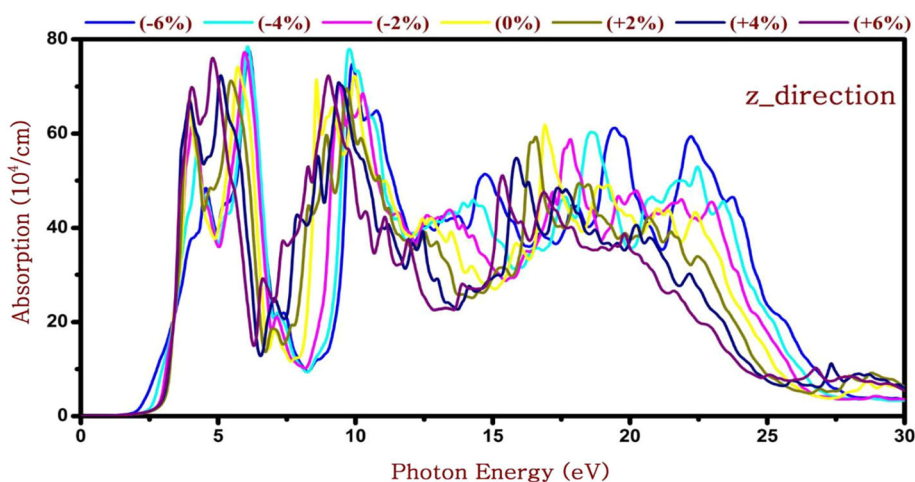


Fig. 9 The absorption of TH-carbon crystal under stress and strain



complex dielectric function increases by increasing the external tensile strain up to 6%. On the other hand by applying compressive strain, this peak slightly decreases. Furthermore, as shown in Fig. 8, the imaginary part of the dielectric function shows also a similar behavior under considered conditions. Generally, by applying both tensile and compressive strains, slight variations are observed in the real and imaginary component of the dielectric function of material.

At last, the absorption of the TH-carbon under the considered strain conditions for the incident lights normal to the monolayer surface is plotted in Fig. 9. According to Fig. 9, by increasing tensile and compressive strains, little red and blue shifts occur in the absorption spectra of the 2D TH-carbon monolayer. The observed optical characteristics for the TH-carbon monolayer suggest this material as a potential material for use as an optical sensor.

4. Conclusions

In summary, by first-principles calculation in the framework of the density functional theory, the electronic and optical properties of the TH-carbon as a new 2D carbon allotrope, which is a direct band gap semiconductor, under biaxial strain condition, are studied. Based on our calculation, TH-carbon is a direct band gap semiconductor with a band gap of 1.65 eV (2.66 eV) obtained from PBE (HSE06) level of theory. Analysis of the electronic aspects indicates that under strain conditions up to -6% compressive strain condition, the energy band gap decreases from 1.65 to 1.11 eV, whereas the tensile strain up to 6% conducts to insignificant changes in the band gap. It is worth noting under effect of stress and strain, this structure remains direct band gap semiconductor as its CBM and VBM are located at the Γ point. Furthermore, our

investigation on the optical properties reveals strain-induced relative shifting in the optical spectra of the monolayer. According to our theoretical finding, it is concluded that this nanostructure may be suitable for usage in electro-optic devices under the considered conditions especially in electronic and optical sensors.

Acknowledgements This work is supported by Kermanshah Branch, Islamic Azad University, Kermanshah, Iran.

References

- [1] K S Novoselov, A K Geim, S V Morozov, D Jiang, Y Zhang, S V Dubonos, et al *Science* **306** 666 (2004)
- [2] S Okada *Physical Review* **B77** 041408 (2008).
- [3] K S Novoselov, A K Geim, S V Morozov, D Jiang, M I Katsnelson, I V Grigorieva, et al *Nature* **438** 197 (2005)
- [4] C Su, H Jiang and J Feng *Physical Review B* **87** 075453 (2013)
- [5] G Mukhopadhyay and H Behera *World J. Eng* **10** 39 (2013)
- [6] J Zhu, D Yang, Z Yin, Q Yan and H Zhang *Small* **10** 3480 (2014).
- [7] C N R Rao, H S S Ramakrishna and Matte U Maitra *Angewandte Chemie International Edition* **52** 13162 (2013)
- [8] M M Obeid *Applied Surface Science* **508** 144824 (2020)
- [9] M M Obeid, H R Jappor, K Al-Marzoki, D M Hoat, T V Vu, S J Edrees, et al *Computational Materials Science* **170** 109201 (2019)
- [10] H T T Nguyen, T V Vua, N T T Binh, D M Hoatd, N V. Hieuf, et al *Chemical Physics* **529** 110543 (2020).
- [11] H R Jappor, M M Obeid, T V Vu, D M Hoat, H D Bui, N N Hieu, et al *Superlattices and Microstructures* **130** 545 (2019)
- [12] D M Hoat, T V Vu, M M Obeid and H R Jappor Tu *Chemical Physics* **527** 110499(2019)
- [13] D M Hoat, T V Vu, M M Obeid and H R Jappor *Superlattices and Microstructures* **130** 354 (2019)
- [14] M Amsler, J A Flores-Livas, L Lehtovaara, F Balima, S A Ghasemi, D Machon, et al *Physical Review Letters* **108** 065501 (2012)
- [15] D Li, K Bao, F Tian, Z Zeng, Z He, B Liu, et al *Physical Chemistry Chemical Physics*, **14** 4347 (2012)
- [16] C He, L Sun, C Zhang, X Peng, K Zhang, and J Zhong *Physical Chemistry Chemical Physics* **14** 8410 (2012)
- [17] C He, L Sun, C Zhang, X Peng, K Zhang and J Zhong *Solid State Communications* **152** 1560 (2012)
- [18] W L Mao, H-k Mao, P J Eng, T P Trainor, M Newville, C-c Kao, et al *Science* **302** 425(2003)
- [19] X-L Sheng, Q-B Yan, F Ye, Q-R Zheng and G Su *Physical Review Letters* **106** 155703(2011)
- [20] J-Q Wang, C-X Zhao, C-Y Niu, Q Sun and Y Jia *Journal of Physics Condensed Matter* **28** 475402 (2016)
- [21] B Ram and H Mizuseki *Carbon* **137** 266 (2018)
- [22] H Alborznia, M Naseri and N Fatahi *Optik* **180** 125 (2019)
- [23] K Novoselov *Nature Materials* **6** 720(2007)
- [24] Z Zhao, F Tian, X Dong, Q Li, Q Wang, H Wang, et al *Journal of the American Chemical Society* **134** 12362 (2012)
- [25] S Zhang, J Zhou, Q Wang, X Chen, Y Kawazoe and P Jena *Proceedings of the National Academy of Sciences* **112** 2372 (2015)
- [26] H Alborznia, M Naseri and N Fatahi *Superlattices and Microstructures* **133** 106217 (2019)
- [27] K S Novoselov, D Jiang, F Schedin, T J Booth, V V Khotkevich, S V Morozov, et al *Proc. Natl. Acad. Sci. U. S. A.* **102** 10451 (2005)
- [28] Z Zheng, M Cox, B Li, J. Mater. Sci. **53** 66 (2018)
- [29] M H Al-Abboodi, F N Ajeel and A M Khudhair *Phys. E Low-dimens. Syst. Nanostruct* **88** 1 (2017)
- [30] P Lambin, H Amara, F Ducastelle and L Henrard *Phys. Rev. B* **86** 045448(2012)
- [31] A A Peyghan, M Noei and M B Tabar *J. Mol. Model* **19** 3007 (2013)
- [32] S F Rastegar, A A Peyghan, and N L Hadipour *Appl. Surf. Sci* **265** 412 (2013)
- [33] J Ortiz-Medina, M L García-Betancourt, X Jia, R Martínez-Gordillo, M A Pelagio-Flores, D. Swanson, et al *Adv. Funct. Mater* **23** 3755 (2013)
- [34] C L Zhang, X Y Wang, W Q Chen and J S Yang *Smart Mater Struct* **26** 025030-1 (2017)
- [35] X Y Dai, F Zhu, Z H Qian and J S Yang *Nano Energy* **43** 22 (2018)
- [36] M Naseri, J Jalilian, F Parandin, K Salehi *Physics Letters A* **382** 2144 (2019)
- [37] M Naseri and S Lin *Chemical Physics Letters* **722** 58-63 (2019)
- [38] M Naseri, S Lin, J Jalilian, J Gu and Z Chen *Frontiers of Physics* **13** 138102 (2018)
- [39] M Naseri *Chemical Physics Letters* **685** 310 (2017)
- [40] H Morshedi, M Naseri, M R Hantehzadeh and S M Elahi *Journal of Electronic Materials* **47**, 2290 (2018)
- [41] M Naseri *Physics Letters A* **382**, 710 (2018)
- [42] M E Kilic and K-R Lee *Carbon* **161** 71 (2020)
- [43] J P Perdew, K Burke and M Ernzerhof *Phys. Rev. Lett* **77** 3865 (1996)
- [44] J Heyd and G E Scuseria *Journal of Chemical Physics* **118** 8207(2003)
- [45] P Blaha, K Schwarz, G K H Madsen, D Kvasnicka, J Luitz and K Schwarz, An augmented PlaneWave + Local Orbitals Program for calculating crystal properties revised edition WIEN2k 13.1 (release 06/26/2013) Wien2K users guide, ISBN 3-9501031-1-2
- [46] H J Monkhorst and J D Pack *Physical Review B* **13** 5188 (1976)
- [47] F Birch *J. Geophys. Res. B* **91** 4949 (1986)
- [48] F Wooten *Optical Properties of Solids, Academic, New York* (1972).
- [49] F Birch *J. Geophys. Res. B* **83** 1257 (1978)
- [50] R. Abt, C. Ambrosch-Draxl and P. Knoll *Physica B Condensed Matter* **194** 196 1451-1452 (1994)
- [51] Y Zhang and W M Shen *Basic of Solid Electronics*, Zhe Jiang University Press, Hangzhou (2005)

Publisher's Note Springer Nature remains neutral with regard to jurisdictional claims in published maps and institutional affiliations.